

## Supporting Information

### **Shaping Protein Amphiphilic Assemblies via Allosteric Effect: From 1D Nanofilament to 2D Rectangular Nanosheet**

Miaomiao Xu,<sup>1,†</sup> Rongjin Zeng,<sup>1,†</sup> Jun Xiang,<sup>2,\*</sup> and Qiang Yan<sup>1,\*</sup>

<sup>1</sup>State Key Laboratory of Molecular Engineering of Polymers, Fudan University, Shanghai 200433, China.

<sup>2</sup>Department of Biomass Science and Engineering, Sichuan University, Chengdu 610065, China.

#### **1. Materials, Methods and Synthetic Procedures.**

**Materials.** L-valine (Sigma, 98%), bis(trichloromethyl) carbonate (Sigma, 99%), 1-(2-aminoethyl)pyrrole-2,5-dione (Sigma, 95%), and P<sup>1</sup>,P<sup>5</sup>-diadenosine-5-pentaphosphate (Ap5A, Sigma, 95%) were all used as received. Wild-type adenylate kinase (AKe) was obtained from *Escherichia coli* as described without any modification and engineering.<sup>1</sup> THF was dried by heating, with sodium strips and calcium hydride respectively, under reflux condition for 3 days. DMF was dried using molecular sieves and then degassed by three freeze-thaw cycles to remove oxygen.

**Methods.** Nuclear magnetic resonance (NMR) was taken by AVANCE III HD 600 MHz of Bruker BioSpin International for characterizing the <sup>1</sup>H- and <sup>31</sup>P-NMR spectra of the polypeptide samples and Ap5A-induced protein amphiphile allosteric effect. Gel electrophoresis (SDS-PAGE) was performed using NuPAGE 4-12% Bis-tris gels with 2-(N-morpholino)ethanesulfonic acid sodium dodecyl sulfate buffer as running buffer. The molecular mass and the molecular weight distribution of polypeptide and protein-polypeptide conjugate samples were measured on a Waters 515 HPLC system equipped with a Waters degasser, a Waters refractive index detector, three Polymer Laboratory PLgel columns. DMF containing 0.10 M LiBr at 30 °C was used as the eluent and near-monodisperse poly(methyl methacrylate) (PMMA) standards were used for calibration.

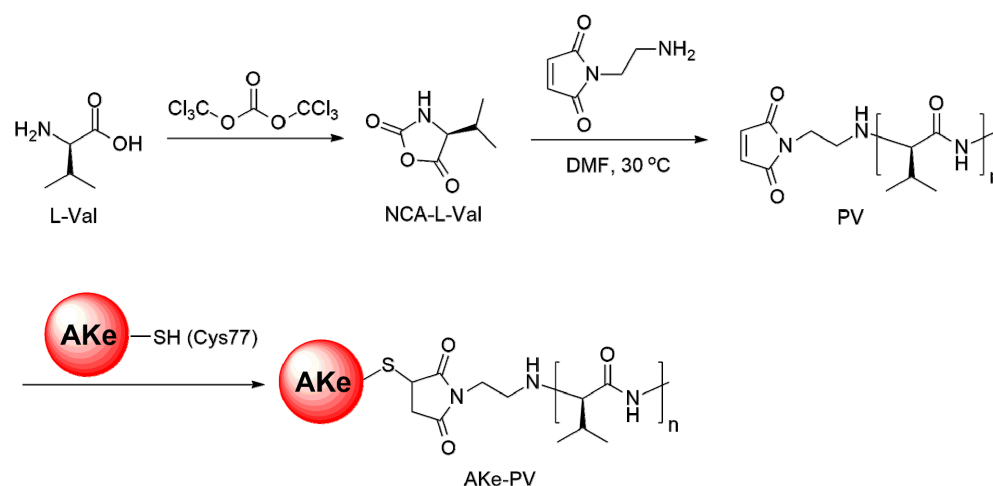
Isothermal titration calorimetry (ITC) experiment was conducted on a MicroCal VP-ITC system at  $293.00 \pm 0.01\text{K}$ , and Ap5A ligand solution ( $1 \times 10^{-5}\text{ M}$ ) was injected into AKe-PV protein amphiphile solution ( $1 \times 10^{-6}\text{ M}$ ) in Tris-HCl buffer ( $\text{pH} = 7.60$ ). The fluorescent experiment was recorded by a HITACHI F-7000 fluorescent spectroscopy (FS) to measure the critical aggregation concentration (CAC) of protein assemblies. Single angle X-ray scattering (SAXS) analysis was conducted by Diamond Light Source on beamline I22 with an X-ray energy of 18 keV. The geometry was calibrated using powdered silver behenate. A 50  $\mu\text{M}$  solution of AKe protein assemblies before and after addition of Ap5A in buffer was measured in a 1.7 mm quartz glass capillary and the scattered X-ray intensity collected. Transmission electron microscopy (TEM) were measured on a FEI Tecnai G2-T20 S-TWIN instrument at a voltage of 120 kV. Atomic force microscope (AFM) were performed from Bruker Dimension-ICON SPM equipped with a J scanner using peak-force mode.

**Sample Preparation.** All the self-assembly processes and allosteric-effect-driven self-assembly shape transformation were carried out in Tris-HCl buffer solution ( $\text{pH} = 7.60$ ) with  $\text{Mg}(\text{NO}_3)_2$  (0.10 mM). AKe-PV protein amphiphile (50  $\mu\text{M}$ ) was dissolved in the buffer and the Ap5A ligand (allosteric modulator) with certain concentrations (5-50  $\mu\text{M}$ ) was added slowly to the protein solution via peristaltic pump under ultrasonication. The aim of sonication here is only to aid the mixing process of AKe-PV and Ap5A ligand, and it had no influence on the self-assembly process. Before and after addition of Ap5A, the final solutions were incubated at room temperature and then observed their self-assembly morphologies via TEM and AFM. To remove the Ap5A from AKe protein, lanthanide (III) bicine complex was added to hydrolyze and cleave the phosphate group of Ap5A,<sup>2</sup> which can recover AKe conformation to open state. In the absence of extra stimuli, the obtained 1D and 2D nanostructures can be stable in solution over one month. However, these nanostructures are susceptible to buffer pH and temperature. When the protein solution is at the acidic ( $\text{pH} < 4.0$ ) or basic ( $\text{pH} > 9.0$ ) condition, since the surface net charge of protein and polypeptide remarkably changes, their aggregated structures are unable to maintain. Because the optimal pH value of AKe protein is neutral (pH

6~8), thus we select the physiological pH environment (pH=7.6) as the experimental condition in all self-assembly process. On the other hand, large temperature fluctuation can also affect this protein self-assembly behavior, overhigh temperature can inhibit the AKe allosteric effect and denature the protein conformation, which can only obtain irregular protein agglomeration.

**Modeling.** The B-factor sharpened map in UCSF Chimera and molecular docking (MD) simulations by using Gromacs package<sup>3</sup> with Amber force field<sup>4</sup> in the NPT ensemble were performed to simulate the AKe-PV protein amphiphilic self-assembly with Ap5A ligand into different protein nanostructures. The time-step was chosen as 5 fs and each simulation was at least conducted for 50 ns. Further, the MD simulations were repeated three times for each system, starting from independent initial configurations.

#### **Synthetic Procedures.**



**Scheme S1.** Synthetic route of protein-polypeptide amphiphilic conjugate (AKe-PV).

#### *Synthesis of L-valine N-carboxyanhydride (NCA-L-Val).*

The synthesis of *L*-valine N-carboxyanhydride (NCA-*L*-Val) monomer was according to the classical method reported in the literature.<sup>5,6</sup> *L*-valine (3.52 g, 30.0 mmol) and bis(trichloromethyl)carbonate (3.53 g, 12.0 mmol) in anhydrous ethyl acetate (100 mL) was added distilled trimethylamine (3.03 g, 30.0 mmol) over 30 s. The mixture was reacted at 50 °C. After 5 h, the reactants were completely soluble and the reaction was cooled down to room temperature. The cyclic monomer (NCA-*L*-Val) was obtained by recrystallization twice from ethyl acetate/hexane (3/1, v/v). Yield: 3.17 g (74%).

$^1\text{H}$  NMR ( $\text{CDCl}_3$ ,  $\delta$ , ppm): 6.42 (brs, -NH-), 4.22 (d, 1H,  $J = 3.9$  Hz, -NH-CH-C=O), 2.23 (m, 1H,  $(\text{CH}_3)_2\text{CH-}$ ), 1.04 (d, 6H,  $J = 6.9$  Hz,  $(\text{CH}_3)_2\text{CH-}$ ).  
ESI-MS: calcd. For  $\text{C}_6\text{H}_9\text{NO}_3$  ( $\text{M}+\text{H}^+$ ), 144.06; found, 144.39.

#### *Synthesis of Maleimide-Terminated Poly(L-valine) (PV).*

The maleimide-terminated poly(L-valine) (PV) was synthesized by the ring-opening polymerization of NCA-L-Val monomer using the initiator of 1-(2-aminoethyl)pyrrole-2,5-dione according to the literature.<sup>7</sup> Typically, maleimide-terminated  $\text{NH}_2$ -initiator (14 mg, 0.1 mmol) was dissolved in anhydrous DMF (8 mL) under dry argon conditions. Then, the cyclic NCA-L-Val monomer (1.72 g, 12 mmol) was added to the flask, and the reaction mixture was preceded for 48 h at 80 °C. The resulting mixture was added dropwise into an excessive amount of ethyl ether and filtered. The residual solvent in the precipitate was removed under vacuum. The obtained polymer was re-dissolved in DMF and dialyzed in deionized water for 48 h using a dialysis tube (MWCO~1.0 kDa). After freeze-drying, white powder of maleimide-terminated poly(L-valine) (PV) was obtained. Conversion: 1.39 g (81%).

$^1\text{H}$  NMR ( $d_6$ -DMSO,  $\delta$ , ppm): 6.86 (s, 2H, -CH=CH-), 4.71 (t, 2H, -N-CH<sub>2</sub>-CH<sub>2</sub>-NH-CO-), 4.47 (s, 84H, -NHCO-CH(CH<sub>3</sub>)-), 3.73 (t, 2H, -N-CH<sub>2</sub>-CH<sub>2</sub>-NH-CO-), 2.02 (s, 84H, -NHCH(CH<sub>3</sub>)-), 0.91 (s, 495H, -CH(CH<sub>3</sub>)<sub>2</sub>).  $M_{w,\text{GPC}} = 12.1$  kDa,  $M_w/M_n = 1.27$ .

#### *Synthesis of Protein-Polypeptide Conjugate (AKe-PV).*

The AKe-PV protein-polypeptide conjugate was obtained by thiol-maleimide Michael addition.<sup>8</sup> Wild-type *Escherichia coli* AKe protein ( $M_w \sim 23$  kDa, 30 mg, 1.3  $\mu\text{mol}$ ) was mixed with PV polypeptide (16 mg, 1.3  $\mu\text{mol}$ ) in nitrogen-purged Tris-HCl buffer (10 mL, pH = 7.6). The reaction solution was stirred at room temperature for 12 h under a nitrogen atmosphere protection. The reaction solution was dialyzed against deionized water with a dialysis tube (MWCO~12 kDa) for 48 h and lyophilized. The product was dissolved in the eluent NaCl (0.1 M) and purified through a gel filtration column. The collected fractions were analyzed by SDS-PAGE and GPC.  $M_{w,\text{GPC}} = 32.5$  kDa,  $M_w/M_n = 1.24$ .

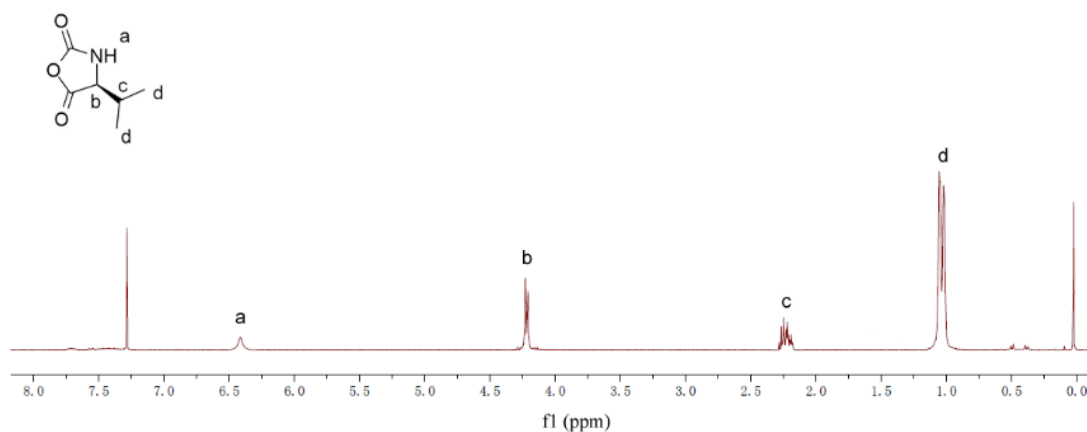


**Figure S1.**  $^1\text{H}$  NMR spectrum of cyclic monomer (NCA-L-Val,  $\text{CDCl}_3$ ).

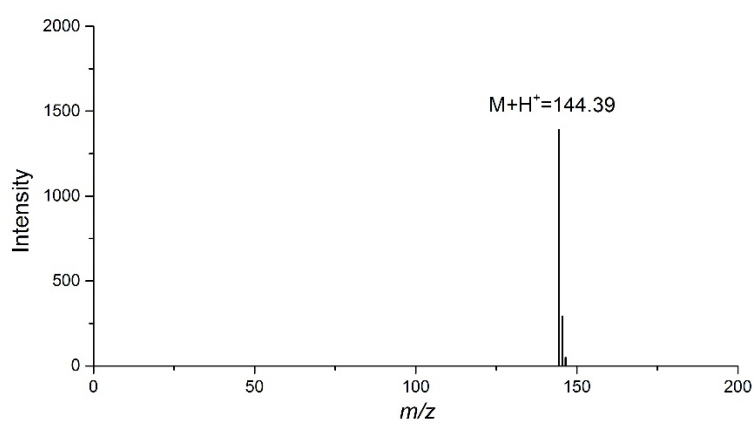


**Figure S2.** ESI-MS spectrum of cyclic monomer (NCA-L-Val).

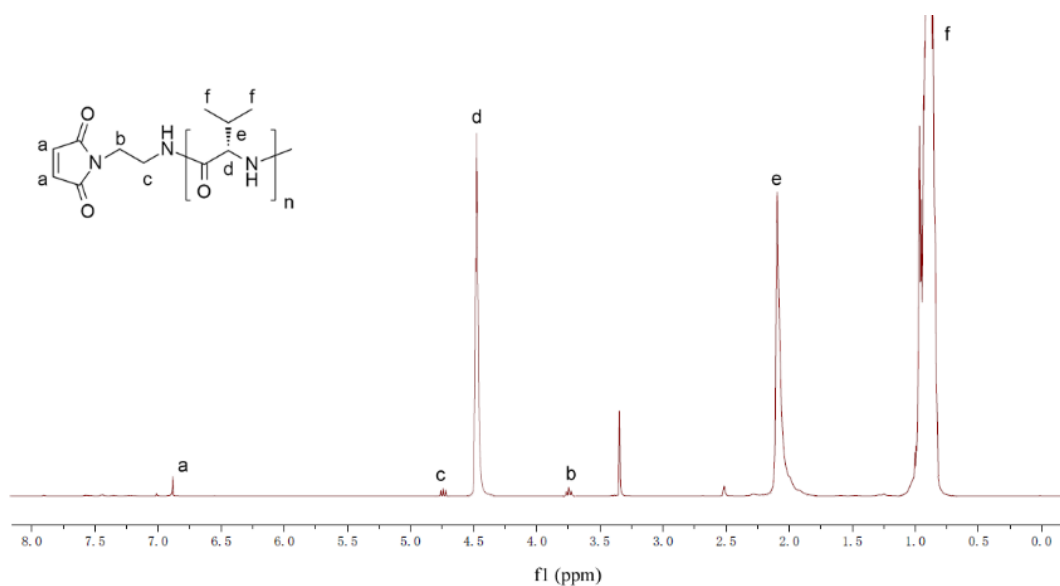


**Figure S3.**  $^1\text{H}$  NMR spectrum of maleimide-terminated poly(L-valine) (PV,  $d_6$ -DMSO).

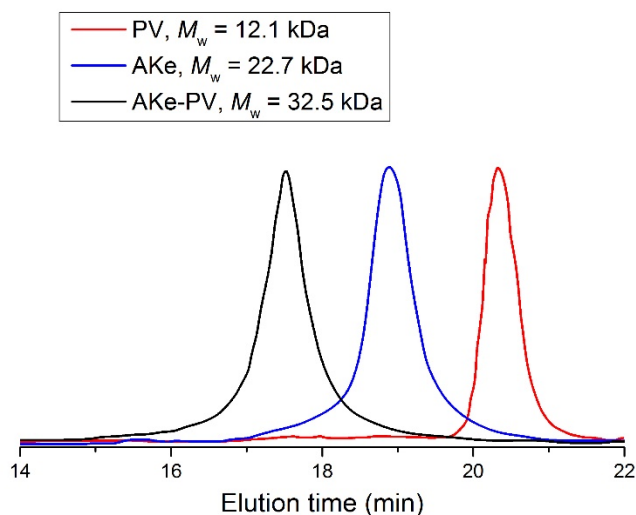


**Figure S4.** GPC curves of pure PV (red), AKe protein (blue) and AKe-PV protein-polypeptide conjugate (black).

About the GPC results, the PV polypeptide and AKe protein showed clear peak at the elution time of 18.9 min and 20.4 min, respectively, corresponding to their weight-average molecular weight ( $M_w$ ) of 12.1 kDa and 22.7 kDa. After conjugation between AKe and PV by thiol-Michael addition, the resulted polymer gave a GPC trace shifted to lower elution time (17.3 min), which corresponds to the  $M_w$  of 32.5 kDa. This value is near the sum of AKe and PV ( $M_w = 12.1 \text{ kDa} + 22.7 \text{ kDa} = 34.6 \text{ kDa}$ , the small deviation is derived from the property differences between protein and selected calibrated standard), indicating the high-efficient coupling reaction.

## 2. Allosteric Binding Affinity of AKe-PV and Ap5A Ligand by ITC.

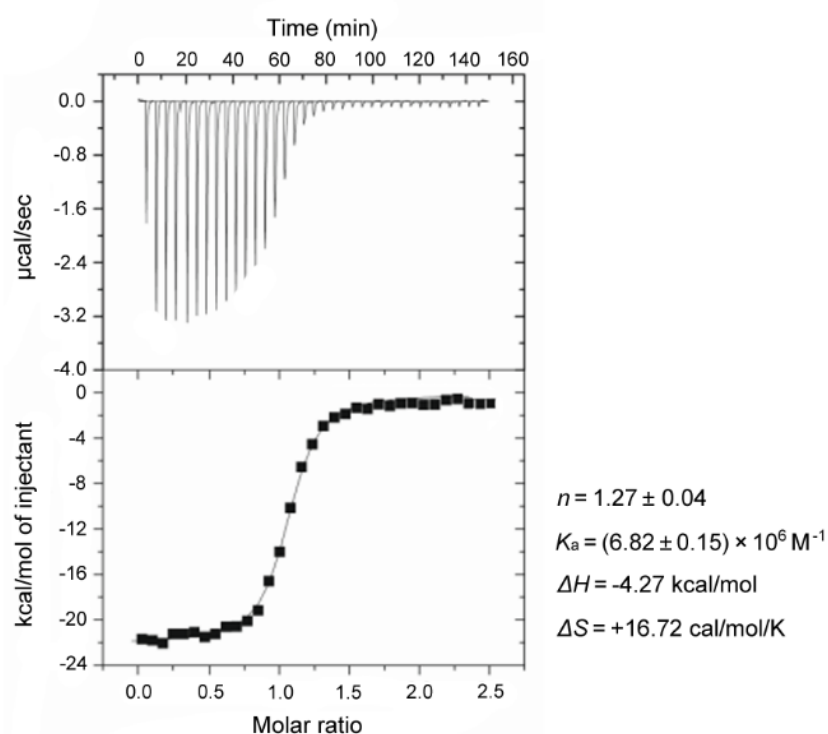


**Figure S5.** ITC data for the allosteric binding affinity between AKe-PV and Ap5A. The binding number is determined to be  $n = 1.27 \pm 0.04$ , the association constant  $K_a = (6.82 \pm 0.15) \times 10^6 \text{ M}^{-1}$ , and the binding enthalpy of  $\Delta H = -4.27 \text{ kcal/mol}$  and the binding entropy of  $\Delta S = +16.72 \text{ cal/mol/K}$ .

### 3. Critical Aggregation Concentration (CAC) and TEM Results of AKe-PV Amphiphile.

AKe-PV was dissolved in deionized water to obtain aqueous solution at concentration of 0.1 mM. Then the high concentrated protein amphiphile solution was diluted to a variety of concentration for further experiments. To measure the critical aggregation concentration (CAC), using pyrene as a fluorescent probe molecule and 0.1  $\mu\text{M}$  of pyrene in acetone (10  $\mu\text{L}$ ) was added to various AKe-PV solution, and then the mixtures were sonication for 20 min before fluorescent emission records. The CAC was chosen as the concentration when pyrene showed an apparent jump in the  $I_3/I_1$  ratio with an increase of AKe-PV concentration, indicating the aggregation of AKe-PV amphiphiles in water.

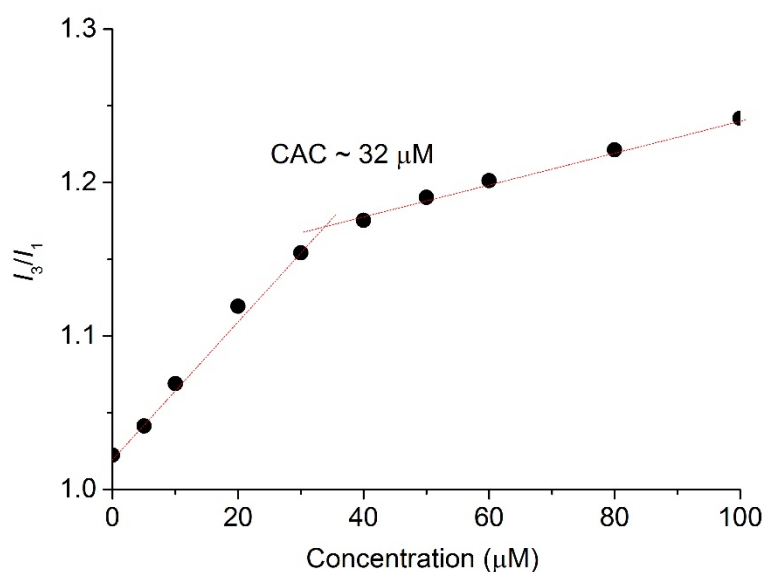


**Figure S6.** Determination of CAC for AKe-PV protein amphiphile by using fluorescent probe method: the CAC is ~0.32  $\mu\text{M}$ .



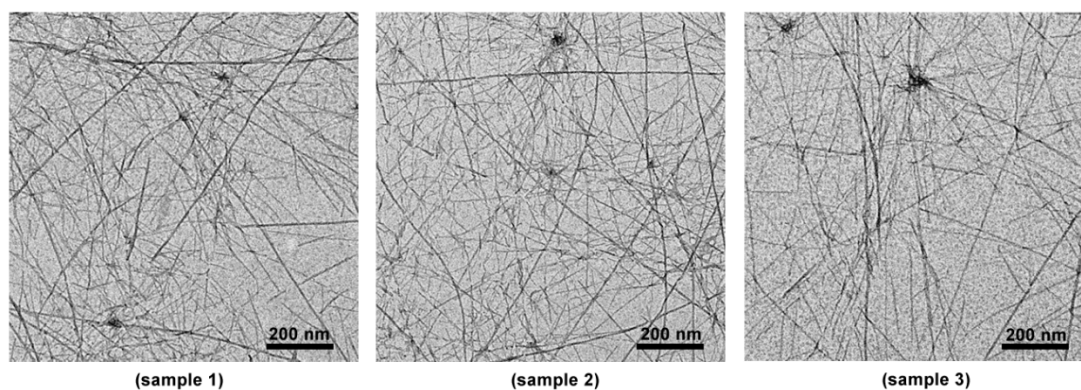


**Figure S7.** The parallel test of different batches of AKe-PV self-assembled structures in aqueous solution to confirm the reproducibility of self-assembly process. The three batches of aggregates at the same conditions all manifested typical nanofilament structure with the same size and shape, indicating that AKe-PV can initially self-assemble into 1D nanostructure.

#### 4. SAXS Analysis of AKe-PV Protein Nanofilament in the Absence of Ap5A Ligand.

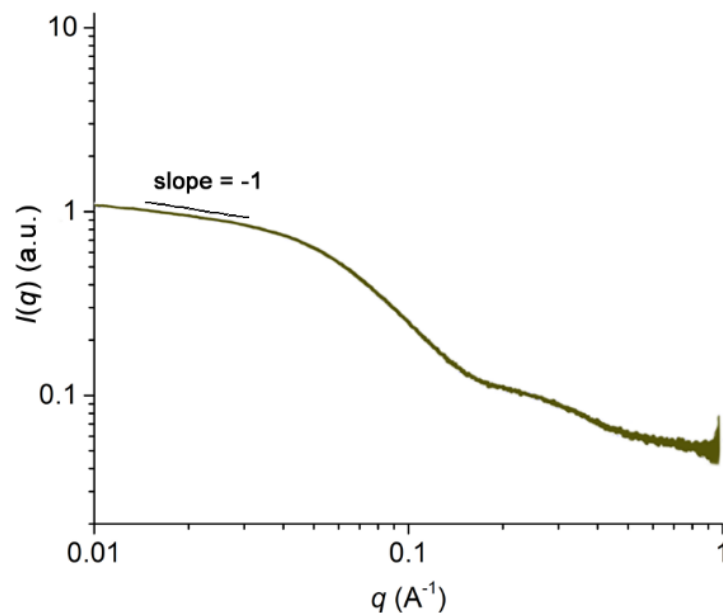


**Figure S8.** SAXS profile plot for solution structures of AKe-PV protein nanosheets in the absence of Ap5A ligand. The logarithmic plotting of scattering data vs  $q$  vector showed a slope of -1, which fits to 1D filamentous nanostructure and is consistent with the TEM and AFM result.

## 5. Computational Simulation of the Protein Nanofilament Structure

### Self-Assembled by AKe-PV Protein Amphiphiles.

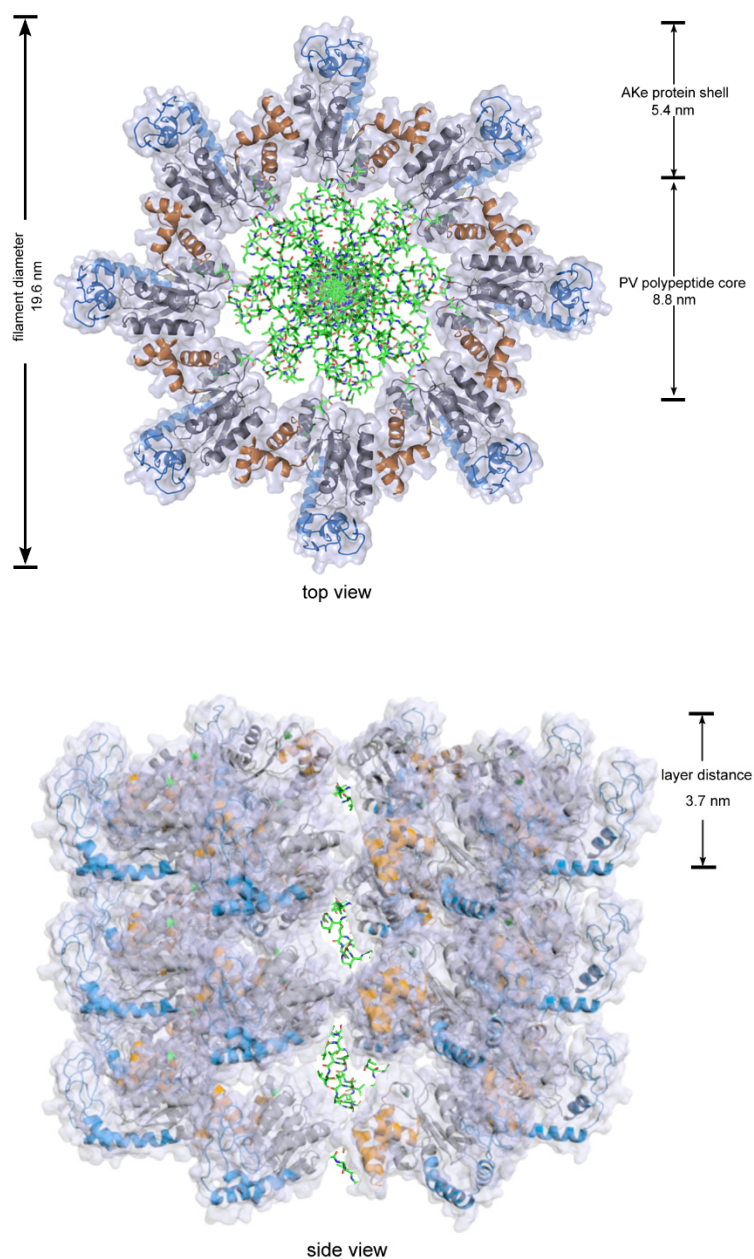


**Figure S9.** Molecule-level self-assembled model of AKe-PV amphiphile into protein nanofilament structure. Top image, top view: the calculated diameter of protein nanofilament is 19.6 nm, in which AKe protein shell accounts for 5.4 nm and PV polypeptide core accounts for 8.8 nm; Bottom image, side view: AKe-PV stacking along 1D direction and thickness of each layers is 3.7 nm. The calculated AKe protein volume is consistent with that of in open conformational state.

## 6. SAXS Analysis of AKe-PV Protein Nanosheet in the Presence of Ap5A Ligand.

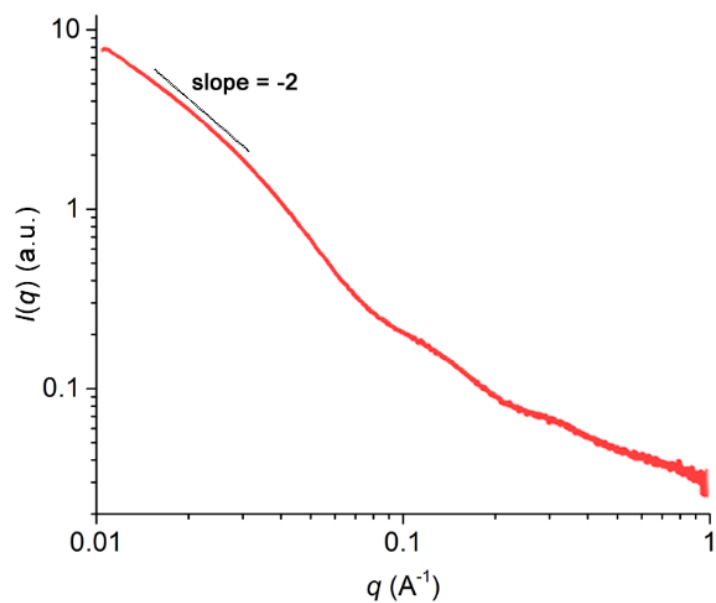


**Figure S10.** SAXS profile plot for solution structures of AKe-PV protein nanosheets in the presence of Ap5A ligand. The logarithmic plotting of scattering data vs  $q$  vector showed a slope of -2, which fits to 2D sheet-like nanostructure and is consistent with the TEM and AFM result.

## 7. Computational Simulation of the 2D Protein Nanosheet Structure Self-Assembled by AKe-PV Protein Amphiphiles in the Presence of Ap5A Ligand.

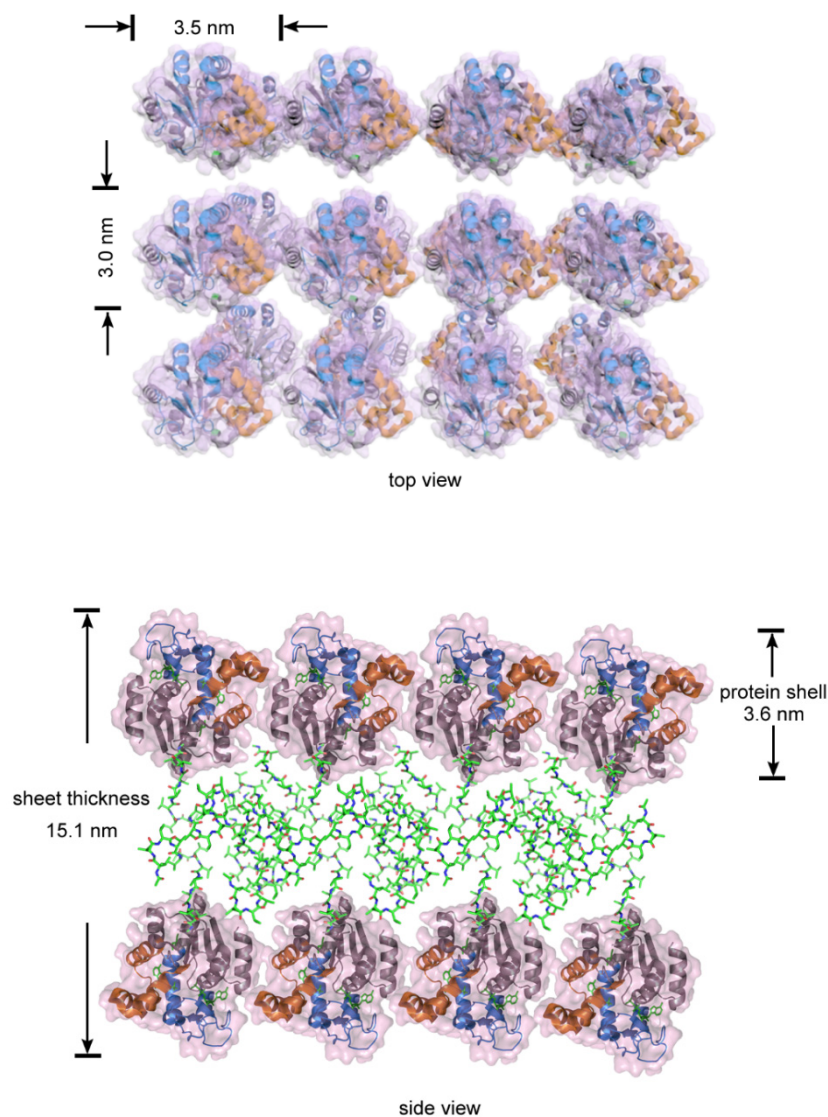


**Figure S11.** Molecule-level self-assembled model of AKe-PV amphiphile into protein nanosheet induced by Ap5A ligand. Top image, top view: the calculated each protein particle in closed conformational state is 3.5 nm×3.0 nm; Bottom image, side view: AKe-PV molecular packing along 2D direction and the thickness of nanosheet is 15.1 nm, in which the protein shell accounts for 3.6 nm. The calculated AKe protein volume is consistent with that of in closed conformational state.

## 8. Reversible Deformation from 2D Nanosheet to 1D Nanofilament.

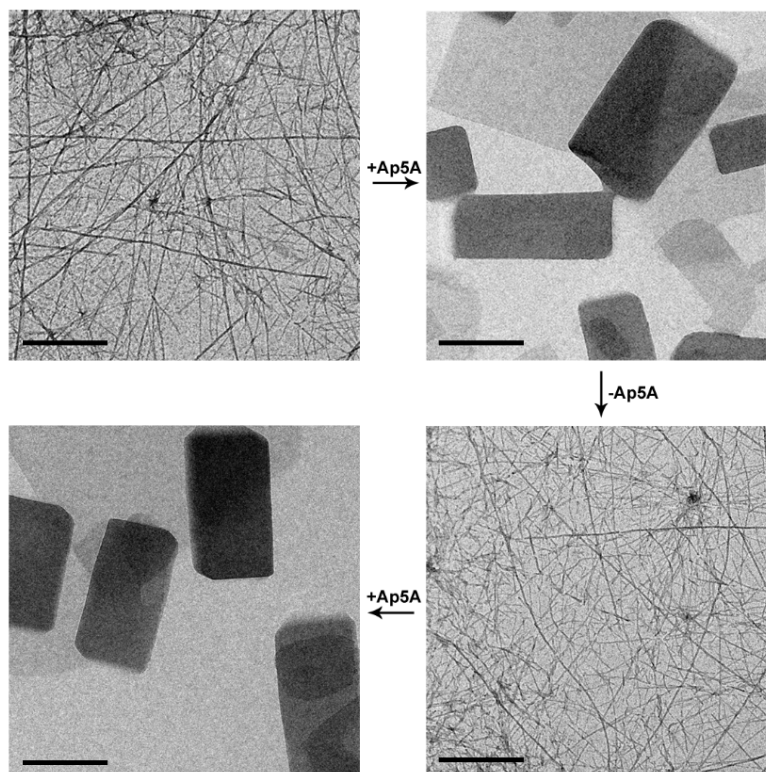


**Figure S12.** Reversible shape transition of AKe-PV amphiphile under the control of Ap5A ligand through reversible protein allostery: initial 1D protein nanofilament (upper left), 2D nanosheet upon Ap5A (upper right), back to 1D protein nanofilament upon removal of Ap5A (low right), and reconstruction of 2D nanosheet with Ap5A (low left). Scale bar is 200 nm.



## 9. The Universality of Allostery-Driven Protein Self-Assembly Shape Transformation.

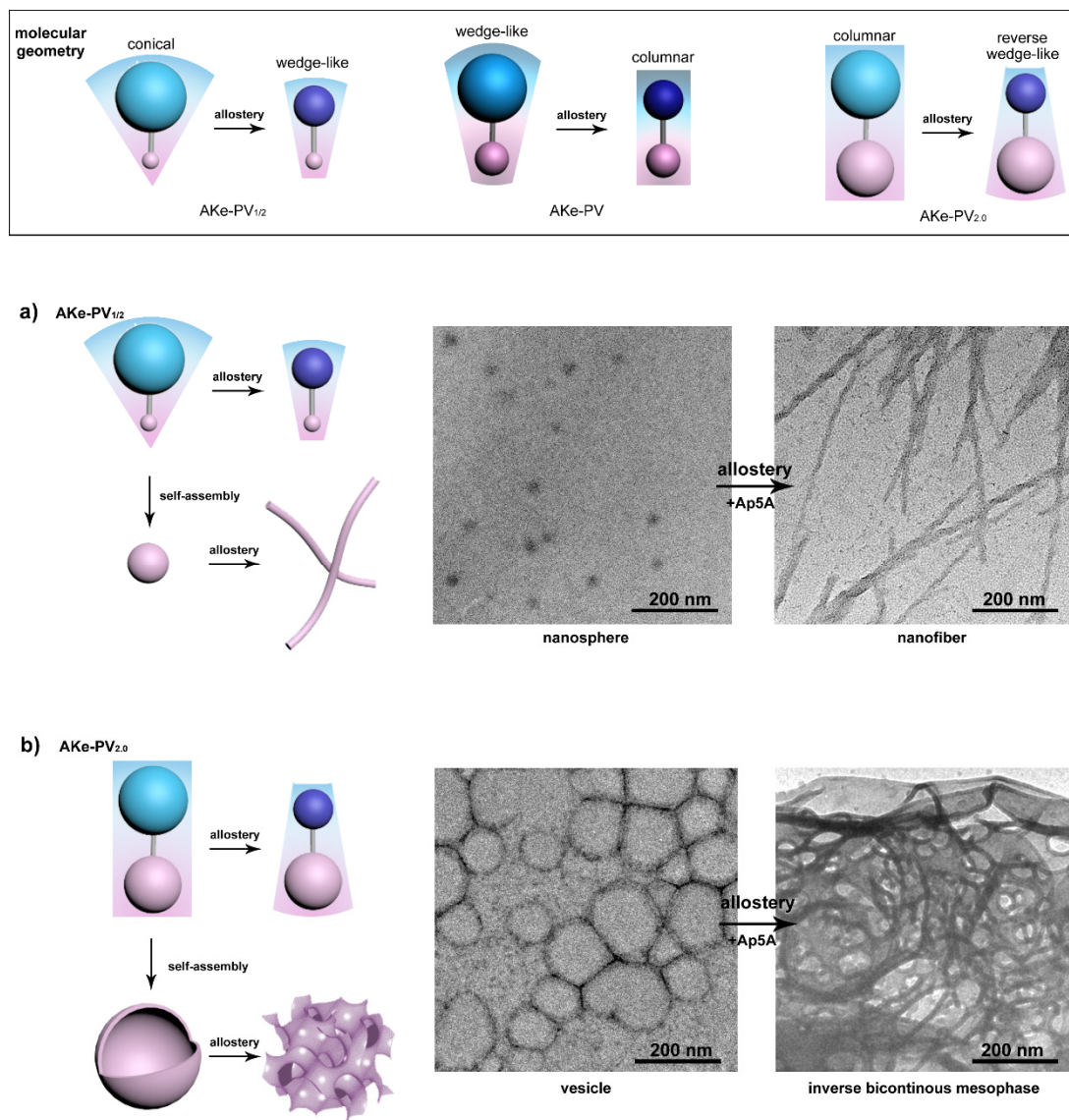


**Figure S13.** Top panel: Molecular geometrical changes of different AKe-PV protein amphiphiles before and after allostery: left, AKe-PV<sub>1/2</sub>; middle, AKe-PV; right, AKe-PV<sub>2.0</sub>. Bottom: (a) Schematic illustration and TEM images showing the morphological transformation of AKe-PV<sub>1/2</sub> assemblies before and after allostery (protein nanosphere → nanofiber); (b) Schematic illustration and TEM images showing the morphological transformation of AKe-PV<sub>2.0</sub> assemblies before and after allostery (protein vesicle → inverse bicontinuous mesophase). The concentrations of AKe-PV amphiphiles were at 50  $\mu$ M and Ap5A allosteric modulator was fixed at 50  $\mu$ M.

## References

- (1) Wolf-Watz, M.; Thai, V.; Henzler-Wildman, K.; Hajipavlou, G.; Eisenmesser, E. Z.; Kern, D. *Nat. Struct. Mol. Biol.* **2004**, *11*, 945-949.
- (2) Calderon, A.; Yatsimirsky, A. K. *Inorg. Chimie Acta.* **2004**, *357*, 3483-3492.
- (3) Spoel, D. V. D.; Lindahl, E.; Hess, B.; Groenhof, G.; Mark, A. E.; Berendsen, H. J. *C. J. Comput. Chem.* **2005**, *26*, 1701-1709.
- (4) Case, D. A.; Cheatham III, T. E.; Darden, T.; Gohlke, H.; Luo, R.; Merz, K. M.; Onufriev, A.; Simmerling, C.; Wang, B.; Woods, R. *J. Comput. Chem.* **2005**, *26*, 1668-1679.
- (5) Wilder, R.; Mobashery, S. *J. Org. Chem.* **1992**, *57*, 2755-2756.
- (6) Yan, Q.; Zhang, H. J.; Zhao, Y. *ACS Macro Lett.* **2014**, *3*, 472-476.
- (7) Song, H. J.; Yang, G.; Huang, P. S.; Kong, D. L.; Wang, W. W. *J. Mater. Chem. B.* **2017**, *5*, 1724-1733.
- (8) Li, M.; De, P.; Li, H.; Sumerlin, B. S. *Polym. Chem.* **2010**, *1*, 854-859.